

# A Finite Element Framework for Some Mimetic Finite Difference Discretizations

C. Rodrigo<sup>a,\*</sup>, F.J. Gaspar<sup>a</sup>, X. Hu<sup>b</sup>, L. Zikatanov<sup>c,d</sup>

<sup>a</sup>*Applied Mathematics Department and IUMA, University of Zaragoza, Spain.*

<sup>b</sup>*Department of Mathematics, Tufts University, Medford, MA, USA.*

<sup>c</sup>*Department of Mathematics, Penn State University, University Park, PA, USA*

<sup>d</sup>*Institute for Mathematics and Informatics, Bulgarian Academy of Sciences, Sofia, Bulgaria*

---

## Abstract

In this work we derive equivalence relations between mimetic finite difference schemes on simplicial grids and modified Nédélec-Raviart-Thomas finite element methods for model problems in  $\mathbf{H}(\mathbf{curl})$  and  $H(\mathbf{div})$ . This provides a simple and transparent way to analyze such mimetic finite difference discretizations using the well-known results from finite element theory. The finite element framework that we develop is also crucial for the design of efficient multigrid methods for mimetic finite difference discretizations, since it allows us to use canonical inter-grid transfer operators arising from the finite element framework. We provide special Local Fourier Analysis and numerical results to demonstrate the efficiency of such multigrid methods.

*Keywords:* Mimetic finite differences, Finite element methods, Nédélec-Raviart-Thomas finite elements, Multigrid, Local Fourier analysis  
*2008 MSC:* 65F10, 65N22, 65N55

---

## 1. Introduction

We consider mimetic finite difference (MFD) methods for problems in  $\mathbf{H}(\mathbf{curl})$  and  $H(\mathbf{div})$  with essential boundary conditions. Such methods are designed in order to have natural discrete analogues of conservation (of mass, momentum, etc), symmetry and positivity of the operators. They are also

---

\*Corresponding author. Phone: +34 976761142; E-mail: carmenr@unizar.es

structure preserving discretizations, namely, they form discrete de Rham complexes.

Such discretization techniques were started in the School of A. A. Samarskii at the Moscow State University, and they have been further developed and analyzed by Shashkov [1] and Vabishchevich [2]. Regarding the MFD methods, our presentation here follows Vabishchevich [2] and his Vector Analysis Grid Operators (VAGO) framework for dual simplicial/polyhedral (Delau-nay/Voronoi) grids.

Many authors have contributed to the research in this field, by applying the MFD methods successfully to several applications ranging from diffusion [3, 4, 5], magnetic diffusion and electromagnetics [6] to continuum mechanics [7] and gas dynamics [8]. We refer to a recent comprehensive review paper by Lipnikov, Manzini, and Shashkov [9] and a recent book by Beirão da Veiga, Lipnikov, and Manzini [10] on the subject for details and literature review.

We are interested in the MFD discretizations of two (standard) model problems in  $\mathbf{H}(\mathbf{curl})$  and  $H(\mathbf{div})$ . We show that the MFD methods can be fitted in a more or less standard finite element (FE) framework which leads to convergence results and makes the design of efficient and fast solvers for the resulting linear systems quite easy. Our approach is somewhat like special discrete Hodge operators and, therefore, is related to the generalized finite difference approach proposed by Bossavit (see e.g. [11] and references therein). We point out that, in the classical finite difference setting, convergence results exist, as can be seen in [2], but deriving them is by all means not an easy task. Moreover, while we provide details on the constructions in 2D, the equivalence between the MFD methods and the FE methods carries over with trivial modifications to 3D case as well. We have only chosen 2D because it makes the exposition much easier to understand.

Such connections between the MFD schemes and the mixed FE methods for diffusion equations with Raviart-Thomas elements have been already established, see [12, 13, 14, 15, 16] and references therein. In fact, designing finite element methods on arbitrary grids is a hot topic and we refer to the recent works on agglomerated grids [17, 18, 19] and virtual finite element methods [20, 21, 22].

Most of the existing works are on approximation, stability and structure preserving properties of the MFD discretizations. Developing fast solvers for the resulting linear systems is a topic that needs more attention, since the design of fast solvers makes the MFD discretizations more practical and

efficient. For FE methods, solvers can be built using the agglomeration techniques introduced by Lashuk and Vassilevski [17, 18]. Such techniques do not apply to the MFD discretizations (even on simplicial grids!) and, to the best of our knowledge, such results are not available in the literature. We point out though that on rectangular grids for standard finite difference schemes for  $H(\text{div})$  problems, a distributive relaxation based multigrid was proposed in [23].

As we have pointed out, our goal is to apply classical multigrid and subspace correction techniques [24, 25, 26, 27, 28] for the mimetic discretizations, by first establishing the relation with Nédélec-Raviart-Thomas elements. Such approach automatically makes efficient methods such as the ones developed by Arnold, Falk and Winther [29] and Hiptmair and Xu (HX) [30] preconditioners applicable for the MFD methods.

Regarding the convergence of  $W$ - and  $V$ -cycle multigrid with a multiplicative Schwarz relaxation proposed in [29], we complement the numerical results with practical Local Fourier Analysis (LFA) which provides sharp estimates of the multigrid convergence rates. We use a variant of LFA that is applicable on simplicial grids (see [31]) and compare the convergence rates predicted by LFA with the actual convergence rates of  $W$ -cycle and  $V$ -cycle multigrid.

The rest of the paper is organized as follows. In Section 2, we describe the MFD schemes on simplicial grids. In Section 3 we derive the “modified” Nédélec-Raviart-Thomas FE methods and show their equivalence to the VAGO MFD schemes. Section 4 defines the multigrid components: smoothers, and, with the help of the results from Section 3, the canonical inter-grid transfer operators. In this section, we also discuss the setup and the design of appropriate LFA for edge-based discretizations and Schwarz smoothers. The results obtained from the LFA analysis are shown in Section 5, together with the convergence rates of the resulting multigrid algorithm. Finally, conclusions are drawn in Section 6.

## 2. Mimetic finite difference discretizations on triangular grids

We consider the following two model problems for  $\mathbf{u}$  in a two dimensional simply connected domain  $\Omega$ :

$$\mathbf{curl} \text{rot } \mathbf{u} + \kappa \mathbf{u} = \mathbf{f}, \quad \text{in } \Omega, \quad (2.1)$$

$$-\mathbf{grad} \text{div } \mathbf{u} + \kappa \mathbf{u} = \mathbf{f}, \quad \text{in } \Omega, \quad (2.2)$$

subject to essential boundary conditions (vanishing tangential or normal components respectively). We also used  $\mathbf{u}$  and  $\mathbf{f}$  to denote solutions and right hand sides for both problems without distinguish them in *different* equations and spaces explicitly. The corresponding variational forms (used in the derivation of the FE scheme) are: Find  $\mathbf{u} \in \mathbf{H}(\mathbf{curl})$  and  $\mathbf{u} \in H(\text{div})$ , respectively, such that

$$(\text{rot } \mathbf{u}, \text{rot } \mathbf{v}) + \kappa(\mathbf{u}, \mathbf{v}) = (\mathbf{f}, \mathbf{v}), \quad \text{for all } \mathbf{v} \in \mathbf{H}(\mathbf{curl}), \quad (2.3)$$

$$(\text{div } \mathbf{u}, \text{div } \mathbf{v}) + \kappa(\mathbf{u}, \mathbf{v}) = (\mathbf{f}, \mathbf{v}), \quad \text{for all } \mathbf{v} \in H(\text{div}). \quad (2.4)$$

In 3D we replace rot with a 3-dimensional **curl**. In the variational form,  $\mathbf{H}(\mathbf{curl})$  and  $H(\text{div})$ , are the spaces of square integrable vector valued functions which also have square integrable rot (**curl** in 3D) or div respectively. The functions in the spaces  $\mathbf{H}(\mathbf{curl})$  and  $H(\text{div})$  are also assumed to satisfy the essential boundary conditions  $(\mathbf{u} \times \mathbf{n}) = 0$  for (2.3) and  $(\mathbf{u} \cdot \mathbf{n}) = 0$  for (2.4) where  $\mathbf{n}$  is the unit normal vector outward to  $\partial\Omega$ .

### 2.1. Mimetic finite differences on a pair of dual meshes

We consider MFD schemes for (2.1) and (2.2) discretized on a pair of primal (Delaunay) simplicial grid and a dual (Voronoi) polyhedral grid. The vertices of the Delaunay triangulation are  $\{\mathbf{x}_i^D\}_{i=1}^{N_D}$ , and the vertices of its dual Voronoi mesh are the circumcenter of the Delaunay triangles. We denote the Voronoi vertices by  $\{\mathbf{x}_k^V\}_{k=1}^{N_V}$ , and note that each such vertex corresponds to a Delaunay triangle  $D_k$ , for  $k = 1, \dots, N_V$ . In Figure 2.1 we have depicted a pair of dual meshes and marked the Delaunay grid-points by squares and the Voronoi grid-points by circles. As is typical in the MFD schemes, we assume that all triangles in the triangulation have only acute angles.

This assumption guarantees that the Voronoi vertices will always be in the

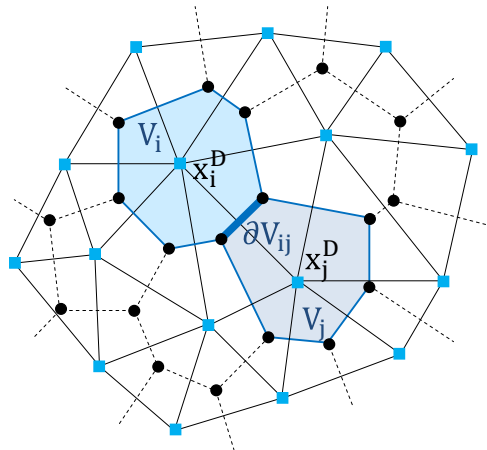


Figure 2.1: A Delaunay mesh and its dual Voronoi mesh.

interior of the Delaunay triangles. For 3D analogues of this assumption we refer to [2]. By duality, to a Delaunay grid point  $\mathbf{x}_i^D$ , there corresponds a Voronoi polygon  $V_i$ ,

$$V_i = \{\mathbf{x} \in \Omega \mid |\mathbf{x} - \mathbf{x}_i^D| \leq |\mathbf{x} - \mathbf{x}_j^D|, j = 1, \dots, N_D, j \neq i\},$$

and we denote the Voronoi edge  $V_{ij} = \partial V_i \cap \partial V_j$ .

We next introduce the spaces of mesh functions associated with the dual Delaunay/Voronoi grids. In an MFD scheme, the unknowns are the components of  $\mathbf{u}$  parallel to the edges of the Delaunay triangulation and evaluated at the middle of these edges. We orient each of the Delaunay edges by the unit vector

$$\mathbf{e}_{ij}^D = \mathbf{e}_{ji}^D, \quad i = 1, \dots, N_D, \quad j \in \mathcal{W}^V(i) = \{j \mid \partial V_{ij} \neq \emptyset, j = 1, \dots, N_D\},$$

which is directed from the node with the smaller index to the node with larger index, see Figure 2.2a. This convention defines a function  $\eta(i, j)$  for every edge  $(\mathbf{x}_i^D, \mathbf{x}_j^D)$ ,

$$\eta(i, j) = \mathbf{n}_i^V \cdot \mathbf{e}_{ij}^D, \quad (2.5)$$

where  $\mathbf{n}_i^V$  is the unit normal vector outward to  $\partial V_i$ . We then denote by  $\mathbf{H}_D$

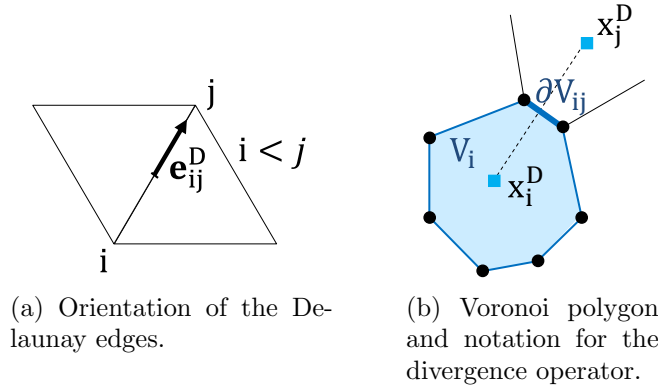


Figure 2.2

the set of mesh functions approximating the values of  $\mathbf{u} \cdot \mathbf{e}_{ij}^D$  at the mid-points of the edges connecting  $\mathbf{x}_i^D$  and  $\mathbf{x}_j^D$ ; namely, for all  $i = 1, \dots, N_D$  and  $j$  such that  $(\mathbf{x}_i^D, \mathbf{x}_j^D)$  is a Delaunay edge we set

$$u_{ij}^D \approx \mathbf{u} \cdot \mathbf{e}_{ij}^D(x_{ij}^D), \quad \mathbf{x}_{ij}^D = \frac{1}{2}(\mathbf{x}_i^D + \mathbf{x}_j^D).$$

To complete the MFD approximation of equations (2.1)-(2.2) we now introduce the spaces of mesh functions associated with the scalar quantities  $\text{rot } \mathbf{u}$  and  $\text{div } \mathbf{u}$ . We modify a little bit of the definitions given in [2] to serve better our purposes, although essentially we do not change anything quantitatively. With the vertices of the Delaunay (resp. Voronoi) grid we associate the space of piece-wise constant functions, which are constants on the polygons of the Voronoi (resp. Delaunay) grid. We set

$$H_D = \{u(\mathbf{x}) \mid u(\mathbf{x}) = u_i^D, \text{ for all } x \in V_i, i = 1, \dots, N_D\}, \quad (2.6)$$

$$H_V = \{u(\mathbf{x}) \mid u(\mathbf{x}) = u_k^V, \text{ for all } x \in D_k, k = 1, \dots, N_V\}. \quad (2.7)$$

In short, the functions in  $H_D$  are constants on Voronoi cells and the functions in  $H_V$  are constants on Delaunay cells. We then define the discrete divergence operator as following:

$$(\text{div}_h \mathbf{u})_i^D := \frac{1}{\text{meas}(V_i)} \sum_{j:V_{ij} \in \partial V_i} u_{ij}^D \text{meas}(V_{ij}), \quad (2.8)$$

where  $\text{meas}(V_i)$  is the area (volume in 3D) of the Voronoi polygon  $V_i$ , and,  $\text{meas}(V_{ij})$ , is the length (area in 3D) of the Voronoi edge (face in 3D) which is dual (perpendicular) to the Delaunay edge  $(\mathbf{x}_i^D, \mathbf{x}_j^D)$ . The relation (2.8) is clearly an analogue of the divergence Theorem on  $V_i$ , namely,

$$\frac{1}{\text{meas}(V_i)} \int_{V_i} \text{div } \mathbf{u} = \frac{1}{\text{meas}(V_i)} \int_{\partial V_i} \mathbf{u} \cdot \mathbf{n}.$$

In a similar fashion we define the discrete operators  $\mathbf{grad}_h : H_D \rightarrow \mathbf{H}_D$ ,  $\text{rot}_h : \mathbf{H}_V \rightarrow H_D$ , and  $\mathbf{curl}_h : H_V \rightarrow \mathbf{H}_D$

$$(\mathbf{grad}_h u)_{ij}^D := (\mathbf{grad}_h u)(\mathbf{x}_{ij}^D) \cdot \mathbf{e}_{ij}^D = \eta(i, j) \frac{u_j^D - u_i^D}{l_{ij}^D}, \quad (2.9)$$

$$(\text{rot}_h \mathbf{u})_k^V = \frac{\eta(i, j) u_{ij}^D l_{ij}^D + \eta(j, l) u_{jl}^D l_{jl}^D + \eta(l, i) u_{li}^D l_{li}^D}{\text{meas}(D_k)}, \quad (2.10)$$

$$(\mathbf{curl}_h u)_{ij}^D = \eta(k, m) \frac{u_k^V - u_m^V}{l_{km}^V}, \quad (2.11)$$

where, in 2D,  $\text{meas}(D_k)$  is the area of the triangle with vertices  $\mathbf{x}_i^D$ ,  $\mathbf{x}_j^D$  and  $\mathbf{x}_l^D$ ;  $l_{ij}^D$ ,  $l_{jl}^D$  and  $l_{li}^D$  are the lengths of its edges, (for example,  $l_{ij}^D = |x_i^D - x_j^D|$ );

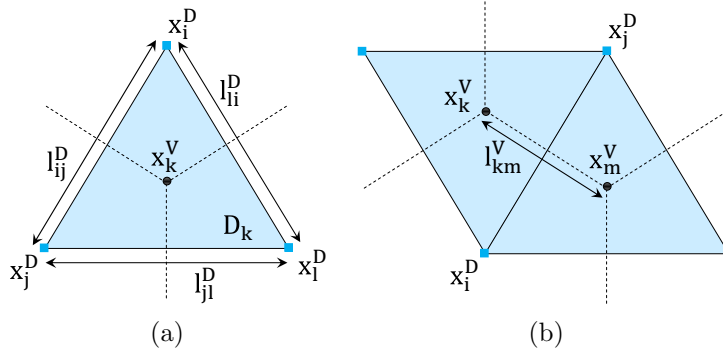


Figure 2.3: Notation used in the definition of  $\text{rot}_h$  and  $\mathbf{curl}_h$  operators

and  $l_{km}^V = |\mathbf{x}_k^V - \mathbf{x}_m^V|$ . We refer to Figure 2.3a-2.3b for clarifying this notation.

Finally, The MFD stencils corresponding to the model problems (2.1)–(2.2) are shown in Figure 2.4a-2.4b for a uniformly refined triangular grid. Note that the stencils match exactly the ones given in [2]. The modifications

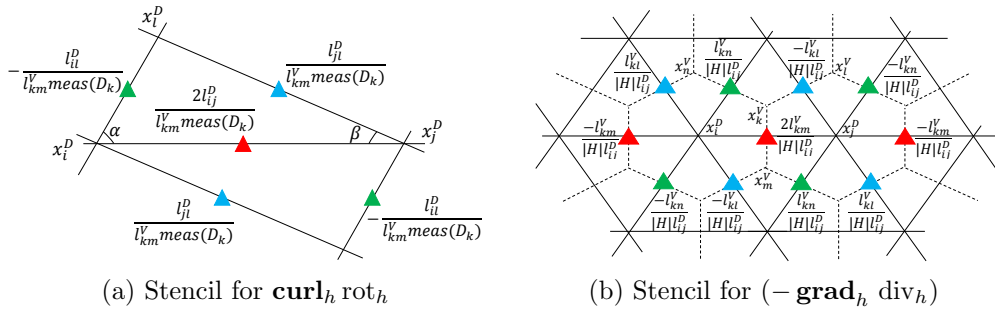


Figure 2.4: Stencils corresponding to a uniformly refined triangular mesh ( $|H| = \text{meas}(V_i)$ )

for the 3D variants of the operators above can also be found in [2]

### 3. Equivalence between mimetic finite differences and finite element methods

In this section, for both model problems (2.1) and (2.2), we are going to introduce suitable FE methods to derive stencils on arbitrary structured

triangular grids that match those obtained by the MFD schemes. The FE methods that we consider are based on the variational formulations (2.3) and (2.4). For definitions of the corresponding Hilbert spaces and results on existence and uniqueness of solutions to these model problems, we refer to [32].

### 3.1. Finite element discretization for (2.3)

Next, we recall that the mesh functions are defined as approximations to the tangential components of the solution on the Delaunay mesh. Therefore, if we would like to construct a FE discretization that matches the MFD method from the previous section, it is reasonable to use lowest order  $\mathbf{H}(\mathbf{curl})$ -conforming Nédélec elements [33, 34] which have the 0-th order moments on the edges of the Delaunay mesh of the tangential components of  $\mathbf{u}$  as degrees of freedom.

In order to approximate the variational problem (2.3) by the lowest-order Nédélec's edge elements, we consider vector valued functions whose restrictions on every Delaunay triangle  $D_k$  are linear in each component and have tangential components that are continuous across the element boundaries. Namely, we define the Nédélec's FE space as following

$$\mathbf{V}_h^N = \{\mathbf{v}_h \in \mathbf{H}(\mathbf{curl}) \mid \mathbf{v}_h|_{D_k} = \begin{bmatrix} a_1 \\ a_2 \end{bmatrix} + b \begin{bmatrix} y \\ -x \end{bmatrix}, k = 1, 2, \dots, N_V\}. \quad (3.1)$$

The FE approximation of (2.3) is: Find  $\mathbf{u}_h \in \mathbf{V}_h^N$  such that

$$(\mathbf{rot} \mathbf{u}_h, \mathbf{rot} \mathbf{v}_h) + \kappa(\mathbf{u}_h, \mathbf{v}_h) = (\mathbf{f}, \mathbf{v}_h), \quad \forall \mathbf{v}_h \in \mathbf{V}_h^N. \quad (3.2)$$

As is well known, the degrees of freedom (functionals which uniquely determine the elements in  $\mathbf{V}_h^N$ ) are chosen to ensure tangential continuity between elements and in the lowest order case, the degrees of freedom are the 0-th order moments of the tangential component on each edge, i.e.  $u_{ij} = \int_{x_i^D}^{x_j^D} \mathbf{u}_h \cdot \mathbf{e}_{ij}^D$ , with  $\mathbf{e}_{ij}^D$  defined as in Section 2.

The bases dual to these degrees of freedom have one basis function per Delaunay edge  $(\mathbf{x}_i^D, \mathbf{x}_j^D)$ ,  $\varphi_{ij} = \frac{1}{2}(\lambda_i \nabla \lambda_j - \lambda_j \nabla \lambda_i)$ , where  $\lambda_i$  and  $\lambda_j$  are the barycentric coordinates of the Delaunay grid. In the standard fashion, the solution of problem (3.2) is written as  $\mathbf{u}_h = \sum_{(i,j)} u_{ij} \varphi_{ij}$ , and the vector of coefficients  $U^N = (u_{ij})$  is a solution to the linear system of equations  $A^N U^N = b^N$ .

Here, the stiffness matrix  $A^N$  has elements given by

$$(A^N)_{(i_2, j_2)(i_1, j_1)} = \sum_{k=1}^{N_V} \int_{D_k} (\text{rot } \varphi_{i_1 j_1} \text{rot } \varphi_{i_2 j_2} + \kappa \varphi_{i_1 j_1} \varphi_{i_2 j_2}) \, \text{d}\mathbf{x}. \quad (3.3)$$

We can now compare the stencil (a row in  $A^N$ ) corresponding to the FE discretization and the MFD discretization derived in Section 2. The result can be seen in Figure 3.1a–3.1b and there is obviously no match. In order

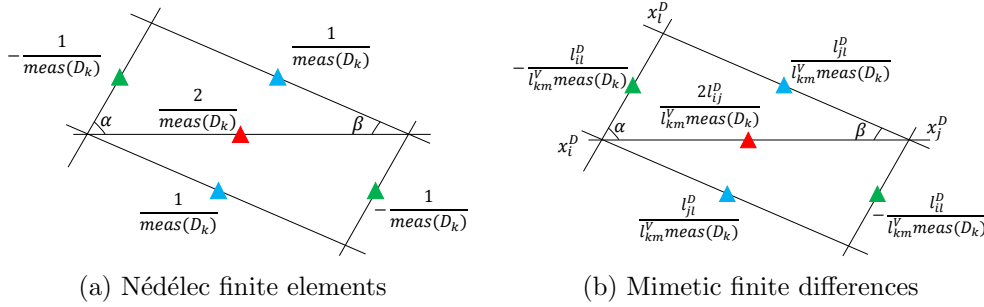


Figure 3.1: Stencils for a general triangulation.

to see the relation between the MFD and the FE stencils, the key is that the MFD degree of freedom  $u_{ij}^D$  is basically a scaled Nédélec FE degree of freedom  $u_{ij}$ , and since the degrees of freedom are dual to the basis functions, we need to scale appropriately the basis in order to have the same entries in the FE stencil. More precisely, if we use the midpoint quadrature rule on every edge (which is exact for functions in  $\mathbf{V}_h^N$ ) we have

$$\mathbf{u}_h(\mathbf{x}) = \sum_{(i,j)} \left( \int_{x_i^D}^{x_j^D} \mathbf{u}_h \cdot \mathbf{e}_{ij}^D \right) \varphi_{ij}(\mathbf{x}) = \sum_{(i,j)} (\mathbf{u}_h \cdot \mathbf{e}_{ij}^D)(x_{ij}^D) l_{ij}^D \varphi_{ij}(\mathbf{x}). \quad (3.4)$$

Hence, an appropriate re-scaling of the basis is  $\varphi_{ij}^s := l_{ij}^D \varphi_{ij}$ . Using the re-scaled basis functions, the corresponding stencil is still not in agreement with the MFD but the resulting rows are proportional to each other. We easily remedy this by scaling also the test functions  $\tilde{\varphi}_{ij} = \frac{1}{l_{km}^V} \varphi_{ij}$ . Summarizing, the MFD matrix  $A^{FD}$  and the FE matrix  $A^N$  satisfy

$$A^{FD} = D_1 A^N D_2, \quad \text{where } \begin{cases} D_1 = \text{diag}((l_{km}^V)^{-1}) \\ D_2 = \text{diag}(l_{ij}^D) \end{cases} \quad (3.5)$$

For the right hand side  $\mathbf{f}$ , in order to be consistent with the FE method, we use the following approximation

$$f_{ij}^D = \frac{1}{l_{km}^V} \int_{\Omega} \mathbf{f} \varphi_{ij} d\mathbf{x}.$$

Then we have  $b^{FD} = D_1 b^N$  and, finally, obtain the following relation between the MFD solution  $U^{FD} = (u_{ij}^D)$  and the Nédélec FE solution given by  $U^N$ :

$$A^{FD} U^{FD} = b^{FD} \implies (D_1 A^N D_2)(U^{FD}) = D_1 b^N, \quad U^{FD} = D_2^{-1} U^N. \quad (3.6)$$

Clearly, there is a function in  $\mathbf{V}_h^N$  corresponding to the MFD solution which we can define as following (in the notation of Section 2)

$$\mathbf{u}_h^{FD}(\mathbf{x}) = \sum_{(i,j)} u_{ij}^D \varphi_{ij}^s(\mathbf{x}).$$

Using the fact that  $U^{FD} = D_2^{-1} U^N$  and  $\varphi_{ij}^s = l_{ij}^D \varphi_{ij}$  we obtain that  $\mathbf{u}_h^{FD} = \mathbf{u}_h$ . As a consequence, from the standard error analysis for the Nédélec FE methods for sufficiently regular  $\Omega$  we automatically have an error estimate and stability for the MFD discretization, namely,

$$\|\mathbf{u} - \mathbf{u}_h^{FD}\|_{\text{rot}} \leq Ch \|\mathbf{f}\|_{L^2(\Omega)}, \quad (3.7)$$

where  $\|\mathbf{v}\|_{\text{rot}} := \sqrt{(\text{rot } \mathbf{v}, \text{rot } \mathbf{v}) + \kappa(\mathbf{v}, \mathbf{v})}$  and  $\|\cdot\|_{L^2(\Omega)}$  is the standard  $L^2$ -norm on  $\Omega$ .

We can also use other approximations of  $\mathbf{f}$  in the MFD schemes. This implies to use an approximation  $\tilde{\mathbf{f}}$  in (3.2) instead of  $\mathbf{f}$ . It is reasonable to assume that  $\|\mathbf{f} - \tilde{\mathbf{f}}\|_{L^2(\Omega)} \leq Ch$ , and, therefore, we still have the error estimate (3.7) by the standard perturbation argument and triangular inequality.

*Remark 1.* Although the matrix  $A^{FD} = D_1 A^N D_2$  could be non-symmetric in the standard Euclidean inner product, it is symmetric in the inner product defined by  $(D_1^{-1} D_2)$ . This is a crucial observation which plays an important role in the design of efficient solvers for the MFD discretizations of problem (2.1).

### 3.2. Finite element methods for (2.2)

The situation with the model problem (2.2) is a bit more involved. To obtain the FE discretization that matches the MFD discretization of (2.2)

we borrow some ideas from [15, 16, 19] and construct an FE space on the polyhedral grid formed by the Voronoi cells. Let us recall that we have  $N_D$  Voronoi cells. We consider the space of functions whose divergence is constant on these cells.

$$\mathbf{V}_h^{\text{RT}} = \{\mathbf{v}_h \in H(\text{div}) \mid \mathbf{v}_h|_{V_i} \in H(\text{div})(V_i), \text{div } \mathbf{v}_h = \text{const.}\}. \quad (3.8)$$

While the particular behavior of the functions inside the Voronoi cell does not matter for our considerations that follow, just to fix the space, we assume that the elements of  $\mathbf{V}_h^{\text{RT}}$  are in the standard Raviart-Thomas space [35, 34] on a sub-triangulation of every Voronoi cell as shown in Figure 3.2 with fixed values of the Raviart-Thomas degrees of freedom on  $\partial V_i$  for  $i = 1, \dots, N_D$ . With this choice, the finite element approximation of (2.4) is: Find  $\mathbf{u}_h \in \mathbf{V}_h^{\text{RT}}$  such that

$$(\text{div } \mathbf{u}_h, \text{div } \mathbf{v}_h) + \kappa(\mathbf{u}_h, \mathbf{v}_h) = (\mathbf{f}, \mathbf{v}_h), \quad \forall \mathbf{v}_h \in \mathbf{V}_h^{\text{RT}}. \quad (3.9)$$

There is one degree of freedom associated with each Voronoi edge  $(\mathbf{x}_k^V, \mathbf{x}_m^V)$ . The corresponding basis functions, dual to these degrees of freedom, are defined using a sub-triangulation of the hexagon as shown in Figure 3.2 (although this is not necessary, see [16]), and then solving an auxiliary finite element problem in each hexagon. We denote by  $RT(H)$  the standard

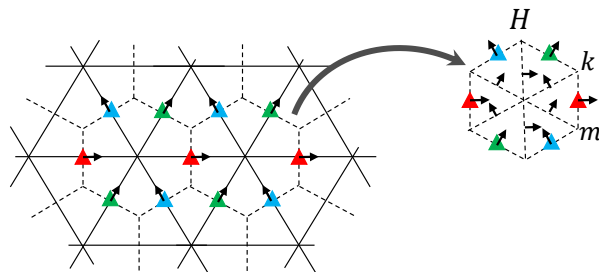


Figure 3.2: Splitting of an hexagon into six triangles to compute the Raviart-Thomas basis function on the hexagon.

Raviart-Thomas space corresponding to a sub-triangulation of a Voronoi cell  $H$ . If we are on a uniformly refined grid, this is a hexagon, which explains why we denoted a generic cell with  $H$ , but in general it is just a convex cell. We restrict our considerations to a hexagon  $H$ , since the other cases are similar. The basis function on  $H$  corresponding to the edge  $(\mathbf{x}_k^V, \mathbf{x}_m^V) \subset \partial H$  is

determined by solving the following constrained minimization problem: Find  $\varphi_{km} \in RT(H)$  ( $\dim RT(H) = 12$ ) such that

$$\left\{ \begin{array}{l} \|\varphi_{km}\|_*^2 \rightarrow \min, \quad \|\varphi_{km}\|_* \simeq \|\varphi_{km}\|_{L^2}, \quad \operatorname{div} \varphi_{km} = \pm \frac{1}{\operatorname{meas}(H)}, \\ \int_{\mathbf{x}_k^V}^{\mathbf{x}_m^V} \varphi_{km} \cdot \mathbf{n}_{jl} = \delta_{(km),(jl)}, \quad \forall jl \in \partial H, \end{array} \right.$$

where  $\|\cdot\|_*$  can be the  $L^2(H)$ -norm or any equivalent norm on the space  $RT(H)$ .

As in the FE discretization of (2.1), which we considered above, to match the MFD discretization, we need to re-scale both the test and trial functions. We set  $\varphi_{km}^s = l_{km}^V \varphi_{km}$ , and take as new test functions  $\tilde{\varphi}_{km} = \frac{1}{l_{ij}^D} \varphi_{km}$ . We then obtain that

$$A^{FD} = D_1 A^{RT} D_2, \quad \text{where} \quad \begin{cases} D_1 = \operatorname{diag}((l_{ij}^D)^{-1}) \\ D_2 = \operatorname{diag}(l_{km}^V) \end{cases} \quad (3.10)$$

Similarly, properly defining the approximation of  $\mathbf{f}$ , we have

$$A^{RT} U^{RT} = b^{RT} \quad \text{and} \quad A^{FD} U^{FD} = b^{FD}$$

with  $b^{FD} = D_1 b^{RT}$ . Together with (3.10), we have  $U^{FD} = D_2^{-1} U^{RT}$ . Therefore, the discrete MFD solution corresponds to the following function in  $\mathbf{V}_h^{RT}$

$$\mathbf{u}_h^{FD}(\mathbf{x}) = \sum_{(k,m)} u_{km}^D \varphi_{km}^s(\mathbf{x}),$$

which also satisfies  $\mathbf{u}_h^{FD} = \mathbf{u}_h$ , namely the MFD solution is also the FE solution. Applying then some standard arguments for a sufficient regular domain  $\Omega$ , we have the following error estimate

$$\|\mathbf{u} - \mathbf{u}_h^{FD}\|_{\operatorname{div}} \leq Ch \|\mathbf{f}\|_{L^2(\Omega)}, \quad (3.11)$$

where  $\|\mathbf{v}\|_{\operatorname{div}} := \sqrt{(\operatorname{div} \mathbf{v}, \operatorname{div} \mathbf{v}) + \kappa(\mathbf{v}, \mathbf{v})}$ .

We can also use other approximation  $\tilde{\mathbf{f}}$  of  $\mathbf{f}$  and, similarly, obtain the error estimate (3.11) by standard perturbation argument and triangular inequality. Moreover, we note that a remark analogous to Remark 1 is necessary here as well.

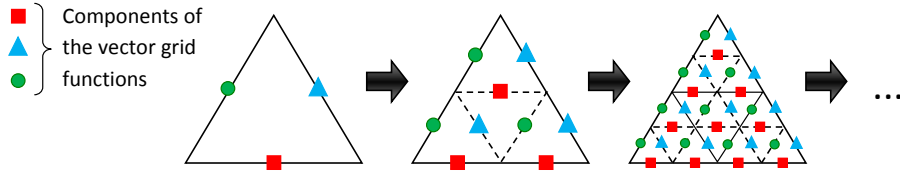


Figure 4.1: Hierarchy of grids to perform the geometric multigrid method, and location of the unknowns

#### 4. Multigrid solvers for mimetic finite differences

Our aim is to find efficient multigrid (MG) methods for the MFD discretization of the vector problems. In this section, we focus on problem (2.1). A geometric multigrid (GMG) method for the MFD discretizations on the Voronoi cells (hexagonal grids) is a topic of our ongoing research and will be reported in our future work. We point out, however, the FE framework that we established in the previous section provides the necessary conditions for applying efficient methods using irregular coarsening strategies and algebraic multigrid together with auxiliary space methods (see [17, 30]). Such methods, however, are not suitable for local Fourier analysis. Since one of our goals is to perform the LFA, we focus on the GMG method for problem (2.1) here.

We are interested in applying a GMG method on triangular grids generated by regular refinement. In this way, we naturally obtain a hierarchy of grids, as shown in Figure 4.1. Next we describe the components for the MG algorithm, i.e., smoother and inter-grid transfer operators.

##### 4.1. Multigrid components

*Smoother.* We use a multiplicative Schwarz smoother proposed in [29] as the relaxation (smoother) in the standard  $V$ - and  $W$ -cycle. This relaxation simultaneously updates all the unknowns around a vertex of the Delaunay grid as shown in Figure 4.2. Overlapping of the unknowns requires non-standard tools in the local Fourier analysis for this smoother.

*Inter-grid transfer operators.* For the transfer of information between two consecutive grids of the hierarchy, canonical inter-grid transfer operators based on the FE framework are constructed. We remind that in order to obtain the Nédélec canonical prolongation, we need to write the coarse-grid

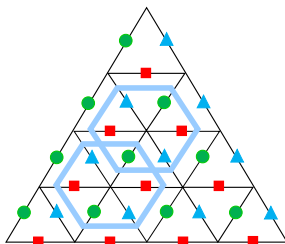


Figure 4.2: Unknowns simultaneously updated in the overlapping block smoother, and overlapping of the blocks.

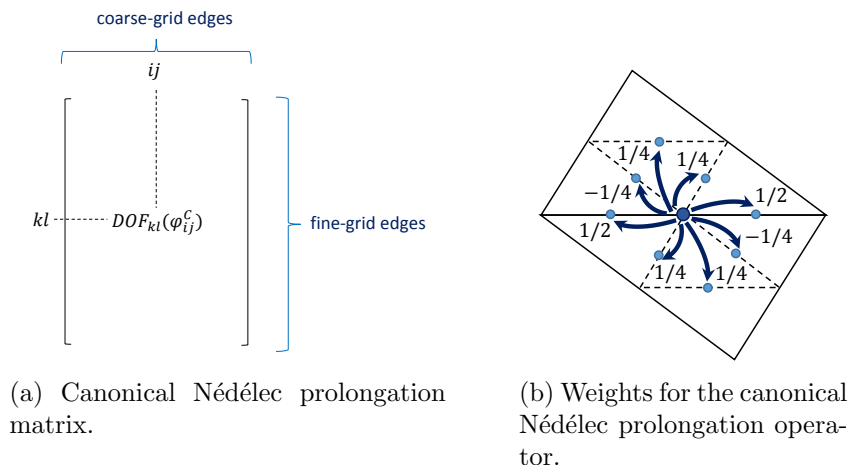


Figure 4.3

basis functions as a linear combination of the fine-grid basis functions, that is,

$$\varphi_{ij}^C = \sum_{kl \in \mathbf{K}} DOF_{kl}(\varphi_{ij}^C) \varphi_{kl}^F,$$

where  $\mathbf{K}$  denotes the set of fine-grid edges inside the support of  $\varphi_{ij}^C$ . In this way, the coefficients in the linear combination are the entries of the prolongation matrix  $P^N$ , i.e.  $(P^N)_{(k,l),(i,j)} = DOF_{kl}(\varphi_{ij}^C)$ , see Figure 4.3a. Moreover, the weights in  $P^N$  are displayed in Figure 4.3b.

Recall that we needed to re-scale the standard Nédélec basis in order to obtain the equivalence between the MFD and FE methods. We modify accordingly the prolongation operator and, from Nédélec canonical prolongation  $P^N$ , we can write everything in terms of the re-scaled fine-grid

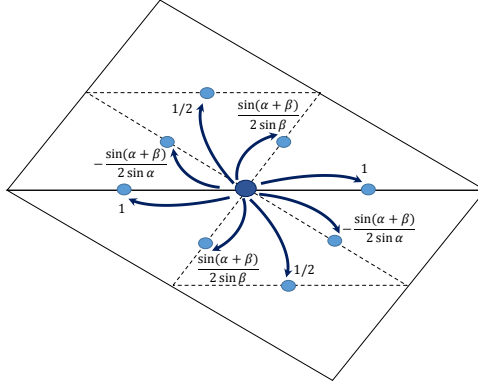


Figure 4.4: Weights for the canonical prolongation associated with the “modified” Nédélec finite element scheme.

and coarse-grid basis functions to obtain that the prolongation matrix is  $P = D_{2,h}^{-1} P^N D_{2,H}$ . The resulting prolongation for a general refined triangle with angles  $\alpha$  and  $\beta$  is given in Figure 4.4. For the restriction, by similar re-scaling, we choose

$$R = D_{1,H}(P^N)^T D_{1,h}^{-1}.$$

It is worth noting here that  $R$  is the adjoint of  $P$  in the inner products induced by  $(D_{1,h}^{-1} D_{2,h})$  and  $(D_{1,H} D_{2,H}^{-1})$  on the fine and coarse grids, respectively, and this agrees with the considerations in Remark 1.

The choice of these inter-grid transfer operators is, in fact, crucial. We emphasize the importance of the relation obtained in Section 3 because without this, it is possible, but, by all means not easy to design efficient GMG methods for these MFD discretizations. Regarding the coarse-grid MFD operator, with this choice of the inter-grid transfer operators, direct discretization on the coarse-grid results in a “Petrov-Galerkin” coarse-grid operator. Namely, note that since  $A_H^N = (P^N)^T A_h^N P^N$ , we have

$$\begin{aligned} A_H^{FD} &= D_{1,H} A_H^N D_{2,H} = D_{1,H} (P^N)^T A_h^N P^N D_{2,H} \\ &= D_{1,H} (P^N)^T \overbrace{D_{1,h}^{-1} D_{1,h}}^I A_h^N \overbrace{D_{2,h} D_{2,h}^{-1}}^I P^N D_{2,H} \\ &= \overbrace{(D_{1,H} (P^N)^T D_{1,h}^{-1})}^R A_h^{FD} \overbrace{(D_{2,h}^{-1} P^N D_{2,H})}^P \\ &= R A_h^{FD} P. \end{aligned}$$

#### 4.2. Local Fourier analysis

We now briefly use local Fourier analysis techniques to assess the convergence of the resulting GMG method. The LFA (or local *mode*) analysis is introduced by A. Brandt in [24] and is a technique based on the Discrete Fourier Transform. To perform this analysis one slightly diverts from the boundary value problem in hand and considers periodic solutions on an infinite regular grid. It is also necessary to have a discrete operator defined with a constant coefficient stencil. The boundary conditions are not taken into account, that is, we assume that the boundary effect is negligible. This, of course, is not true in general, but in many practical situations the LFA gives sharp estimates on the MG convergence rates.

In the framework of LFA, the current approximation to the solution and the corresponding error can be represented by formal linear combinations of discrete *Fourier modes* forming the *discrete Fourier space*. The LFA then identifies invariant subspaces in the Fourier space and studies how multigrid components act on these subspaces. A detailed explanation of all varieties of local Fourier analysis can be found in [26, 36] and on triangular grids, in [31].

We now move on to describe the difficulties in performing LFA for the GMG components defined above. The LFA for our case is indeed nonstandard and we need to deal with several issues described below.

*Simplicial grids.* Local Fourier analysis has been traditionally performed for finite difference discretizations on structured rectangular grids. This analysis was extended to FE discretizations on general structured triangular [37, 38] and tetrahedral [39] grids. The key fact for this extension is to consider an expression of the Fourier transform in new coordinate systems in space and frequency variables and introduce a non-orthogonal unit basis of  $\mathbb{R}^d$ , chosen to fit the geometry of the given simplicial mesh. The basis corresponding to the frequencies space is taken as its reciprocal basis and with these settings the LFA on simplicial grids is not very different from the LFA on the standard rectangular grids.

*Edge-based unknowns.* As we saw, the unknowns in MFD discretizations of problem (2.1) are located at different types of grid-points, and therefore the stencils (the rows of the matrix  $A^{FD}$ ) involve not one, but several different stencils. The key is to split the infinite grid into several different subgrids in such a way that all nodes belonging to a subgrid have the same stencil, and to define suitable grid-functions playing the role of the Fourier modes

for such edge-based discretizations. We refer the reader to [40] for a detailed description of such analysis.

*Overlapping Schwarz smoothers.* Overlapping block smoothers require a special LFA strategy. Classical approaches fail for this class of smoothers, because an overlapping smoother updates some variables more than once, due to the overlapping. The main difficulty is that in addition to the initial and final errors, some intermediate errors appear, and this has to be taken into account in the analysis. To our knowledge, there are only few papers dealing with LFA for overlapping smoothers, and all of them for discretizations on rectangular grids (see [41], [42] and [43]). In [31] this analysis is developed for FE discretizations on triangular grids and in [44], a general LFA technique on simplicial grids for overlapping smoothers is presented.

## 5. Numerical results

In this section, we demonstrate the efficiency of the GMG method for the MFD discretizations based on the multiplicative Schwarz smoother and the inter-grid transfer operators obtained from the modified Nédélec FE discretization. We also show a local Fourier analysis for this kind of discretizations to confirm the experimental results.

We first consider problem (2.1) with  $\kappa = 1$  on an equilateral triangular domain of unit side-length. In Table 1, we display the smoothing factor  $\mu$  and the two-grid  $\rho_{2g}$  convergence factors predicted by the LFA, together with the asymptotic convergence factor computed by using a  $W$ -cycle on a target fine-grid obtained after 10 refinement levels. Since in practice it is worth to know if we can use  $V$ -cycles instead of  $W$ -cycles, due to the high computational cost of the latter, we also show the three-grid convergence factors  $\rho_{3g}$  predicted by LFA for  $V$ -cycles, together with the asymptotic convergence factors experimentally obtained. These results are presented for different numbers of smoothing steps  $\nu$ . From the results in Table 1, we observe accurate predictions of the asymptotic convergence factors. Moreover, an optimal behavior of  $V$ -cycle is shown, since the obtained  $V$ -cycle convergence rates are very similar to the  $W$ -cycle convergence rates. We have seen that in this case, the convergence factors are independent of how the smoothing steps are distributed, and therefore we do not distinguish different distributions in the table. Notice that very good convergence factors, below 0.1, are obtained by using a  $V$ -cycle with only three smoothing steps.

$\nu$	$\mu^\nu$	$W$ -cycle		$V$ -cycle	
		$\rho_{2g}$	$\rho_h^W$	$\rho_{3g}$	$\rho_h^V$
1	0.462	0.331	0.330	0.337	0.334
2	0.214	0.124	0.124	0.133	0.132
3	0.099	0.070	0.069	0.072	0.071
4	0.046	0.045	0.045	0.052	0.052

Table 1: Smoothing ( $\mu$ ), two-grid ( $\rho_{2g}$ ) and three-grid ( $\rho_{3g}$ ) LFA convergence factors, together with measured  $W$ -cycle and  $V$ -cycle asymptotic convergence rates,  $\rho_h^W$  and  $\rho_h^V$ , respectively, for an equilateral triangle and different numbers of smoothing steps,  $\nu$ .

Next, in Figure 5.1, we display the history of the MG convergence for different fine grids. We use a  $V(2, 1)$ -cycle and the stopping criterion is to reduce the initial residual by a factor of  $10^{-10}$ . As is a well-known property of the MG methods, we observe the  $h$ -independent convergence behavior.

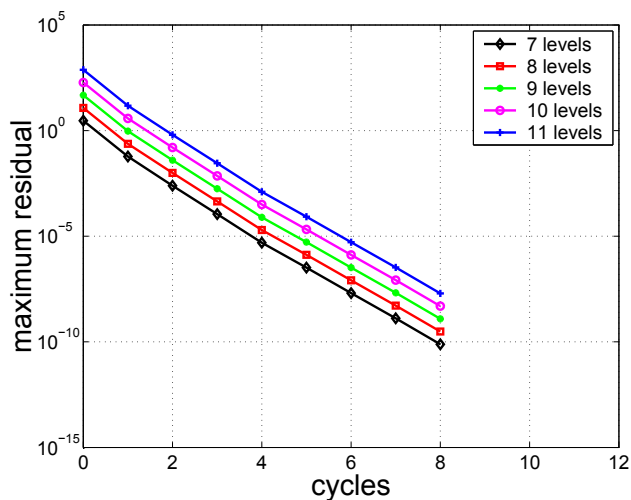


Figure 5.1: History of the multigrid convergence of a  $V(2, 1)$ -cycle for different numbers of refinement levels.

To study the robustness of the proposed method with respect to parameter  $\kappa$ , in Table 2, we show the smoothing and three-grid convergence factors, for both  $W$ - and  $V$ -cycle, predicted by LFA for different values of  $\kappa$  and by

$\kappa$	$\mu$	$W$ -cycle ( $\rho_{3g}^W$ )	$V$ -cycle ( $\rho_{3g}^V$ )
1	0.099	0.070	0.072
$10^{-2}$	0.099	0.070	0.072
$10^{-4}$	0.099	0.070	0.072
$10^{-6}$	0.099	0.070	0.072
$10^{-8}$	0.099	0.070	0.072

Table 2: Smoothing ( $\mu$ ) and three-grid LFA convergence factors by using  $W$ -cycle ( $\rho_{3g}^W$ ) and  $V$ -cycle ( $\rho_{3g}^V$ ) for an equilateral triangular grid, with three smoothing steps ( $\nu = 3$ ), and different values of parameter  $\kappa$ .

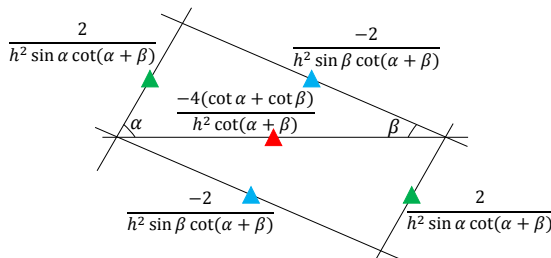


Figure 5.2: Stencil of **curl**-rot operator for an arbitrary triangulation characterized by angles  $\alpha$  and  $\beta$  by using mimetic finite differences.

using three smoothing steps. From the table, it is clear that the results are independent of  $\kappa$ .

To show a more general applicability of the method, arbitrary structured triangular grids are considered. These grids can be characterized by two angles  $\alpha$  and  $\beta$ , and therefore, after simple computations we can obtain the stencil corresponding to **curl**-rot operator in terms of  $\alpha$  and  $\beta$ , as we can see in Figure 5.2.

In this way, a systematic analysis with the LFA tool can be performed for a wide range of triangulations. In Figure 5.3, we display the three-grid convergence factors predicted by the LFA for a wide range of triangular grids characterized by angles  $\alpha$  and  $\beta$ . For these results, a  $V$ -cycle with three smoothing steps has been considered.

From Figure 5.3, we observe a deterioration of the convergence factor when a small angle appears in the triangulation. This behavior is typical when point-wise smoothers are considered on a grid with anisotropy. It is

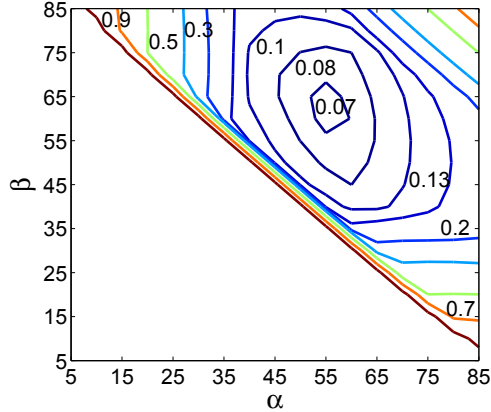


Figure 5.3: Three-grid convergence factors for  $V$ -cycle predicted by LFA for a wide range of triangles characterized by angles  $\alpha$  and  $\beta$ .

possible to improve these convergence factors by using a relaxation parameter  $\omega$ . For example, if an isosceles triangular grid with angles  $80^\circ$ - $80^\circ$ - $20^\circ$  is considered, we obtain a factor of  $\rho_{3g}^V = 0.508$ , but we can improve this result to  $\rho_{3g}^V = 0.252$  by considering a relaxation parameter  $\omega = 1.35$ . These optimal parameters can be obtained for other triangulations by using the LFA. Of course, other well-known techniques can be applied to overcome the difficulties arising from the anisotropy of the grid, such as line-type smoothers, but this is not the focus of this work.

## 6. Conclusions

In this work, we showed an equivalence between the MFD schemes on simplicial grids and some modified FE methods. This relation has been obtained for two model problems in  $\mathbf{H}(\mathbf{curl})$  and  $H(\mathbf{div})$ . This connection leads to immediate convergence results for the MFD schemes and also allows the construction of efficient multilevel methods using the FE framework. Based on the LFA, we theoretically predicted and numerically showed the robustness and the efficiency of the GMG method in  $\mathbf{H}(\mathbf{curl})$  for edge-based discretizations on simplicial grids.

## Acknowledgements

The work of Francisco J. Gaspar and Carmen Rodrigo is supported in part by the Spanish project FEDER /MCYT MTM2013-40842-P and the DGA (Grupo consolidado PDIE). The research of Ludmil Zikatanov is supported in part by NSF DMS-1217142 and NSF DMS-1418843. Carmen Rodrigo gratefully acknowledges the hospitality of the Department of Mathematics of The Pennsylvania State University, where this research was partly carried out.

## References

### References

- [1] M. Shashkov, Conservative finite-difference methods on general grids, Symbolic and Numeric Computation Series, CRC Press, Boca Raton, FL, ISBN 0-8493-7375-1, with 1 IBM-PC floppy disk (3.5 inch; HD), 1996.
- [2] P. N. Vabishchevich, Finite-difference approximation of mathematical physics problems on irregular grids, *Comput. Methods Appl. Math.* 5 (3) (2005) 294–330 (electronic), ISSN 1609-4840, doi:10.2478/cmam-2005-0015, URL <http://dx.doi.org/10.2478/cmam-2005-0015>.
- [3] J. Hyman, M. Shashkov, S. Steinberg, The numerical solution of diffusion problems in strongly heterogeneous non-isotropic materials, *J. Comput. Phys.* 132 (1) (1997) 130–148, ISSN 0021-9991, doi:10.1006/jcph.1996.5633, URL <http://dx.doi.org/10.1006/jcph.1996.5633>.
- [4] J. E. Morel, R. M. Roberts, M. J. Shashkov, A local support-operators diffusion discretization scheme for quadrilateral  $r$ - $z$  meshes, *J. Comput. Phys.* 144 (1) (1998) 17–51, ISSN 0021-9991, doi:10.1006/jcph.1998.5981, URL <http://dx.doi.org/10.1006/jcph.1998.5981>.
- [5] M. Shashkov, S. Steinberg, Solving diffusion equations with rough coefficients in rough grids, *J. Comput. Phys.* 129 (2) (1996) 383–405, ISSN 0021-9991, doi:10.1006/jcph.1996.0257, URL <http://dx.doi.org/10.1006/jcph.1996.0257>.

- [6] J. M. Hyman, M. Shashkov, Mimetic discretizations for Maxwell's equations and the equations of magnetic diffusion, *Progress in Electromagnetic Research* 32 (2001) 89–121.
- [7] L. G. Margolin, M. Shashkov, P. K. Smolarkiewicz, A discrete operator calculus for finite difference approximations, *Comput. Methods Appl. Mech. Engrg.* 187 (3-4) (2000) 365–383, ISSN 0045-7825, doi:10.1016/S0045-7825(00)80001-8, URL [http://dx.doi.org/10.1016/S0045-7825\(00\)80001-8](http://dx.doi.org/10.1016/S0045-7825(00)80001-8).
- [8] J. C. Campbell, M. J. Shashkov, A tensor artificial viscosity using a mimetic finite difference algorithm, *J. Comput. Phys.* 172 (2) (2001) 739–765, ISSN 0021-9991, doi:10.1006/jcph.2001.6856, URL <http://dx.doi.org/10.1006/jcph.2001.6856>.
- [9] K. Lipnikov, G. Manzini, M. Shashkov, Mimetic finite difference method, *J. Comput. Phys.* 257 (part B) (2014) 1163–1227, ISSN 0021-9991, doi:10.1016/j.jcp.2013.07.031, URL <http://dx.doi.org/10.1016/j.jcp.2013.07.031>.
- [10] L. Beirão da Veiga, K. Lipnikov, G. Manzini, The Mimetic Finite Difference Method fo Elliptic Problems, vol. 11 of *Modeling, Simulation & Applications*, Springer-Verlag, Berlin, 2014.
- [11] A. Bossavit, Discretization of electromagnetic problems: the generalized finite differences approach, *Handbook of numerical analysis* 13 (2005) 105–197.
- [12] M. Berndt, K. Lipnikov, D. Moulton, M. Shashkov, Convergence of mimetic finite difference discretizations of the diffusion equation, *East-West J. Numer. Math.* 9 (4) (2001) 265–284, ISSN 0928-0200.
- [13] M. Berndt, K. Lipnikov, M. Shashkov, M. F. Wheeler, I. Yotov, A mortar mimetic finite difference method on non-matching grids, *Numer. Math.* 102 (2) (2005) 203–230, ISSN 0029-599X, doi:10.1007/s00211-005-0631-4, URL <http://dx.doi.org/10.1007/s00211-005-0631-4>.
- [14] F. Brezzi, K. Lipnikov, M. Shashkov, Convergence of the mimetic finite difference method for diffusion problems on polyhedral meshes, *SIAM J. Numer. Anal.* 43 (5) (2005) 1872–1896 (electronic), ISSN 0036-1429, doi:10.1137/040613950, URL <http://dx.doi.org/10.1137/040613950>.

- [15] Y. Kuznetsov, S. Repin, New mixed finite element method on polygonal and polyhedral meshes, *Russian J. Numer. Anal. Math. Modelling* 18 (3) (2003) 261–278, ISSN 0927-6467, doi:10.1163/156939803322380846, URL <http://dx.doi.org/10.1163/156939803322380846>.
- [16] Y. Kuznetsov, S. Repin, Mixed finite element method on polygonal and polyhedral meshes, in: *Numerical mathematics and advanced applications*, Springer, Berlin, 615–622, 2004.
- [17] I. V. Lashuk, P. S. Vassilevski, Element agglomeration coarse Raviart-Thomas spaces with improved approximation properties, *Numer. Linear Algebra Appl.* 19 (2) (2012) 414–426, ISSN 1070-5325, doi:10.1002/nla.1819, URL <http://dx.doi.org/10.1002/nla.1819>.
- [18] I. V. Lashuk, P. S. Vassilevski, The construction of the coarse de Rham complexes with improved approximation properties, *Comput. Methods Appl. Math.* 14 (2) (2014) 257–303, ISSN 1609-4840, doi:10.1515/cmam-2014-0004, URL <http://dx.doi.org/10.1515/cmam-2014-0004>.
- [19] J. E. Pasciak, P. S. Vassilevski, Exact de Rham sequences of spaces defined on macro-elements in two and three spatial dimensions, *SIAM J. Sci. Comput.* 30 (5) (2008) 2427–2446, ISSN 1064-8275, doi:10.1137/070698178, URL <http://dx.doi.org/10.1137/070698178>.
- [20] L. Beirão da Veiga, F. Brezzi, A. Cangiani, G. Manzini, L. D. Marini, A. Russo, Basic principles of virtual element methods, *Math. Models Methods Appl. Sci.* 23 (1) (2013) 199–214, ISSN 0218-2025, doi:10.1142/S0218202512500492, URL <http://dx.doi.org/10.1142/S0218202512500492>.
- [21] L. Beirão da Veiga, F. Brezzi, L. D. Marini, A. Russo, The hitchhiker’s guide to the virtual element method, *Math. Models Methods Appl. Sci.* 24 (8) (2014) 1541–1573, ISSN 0218-2025, doi:10.1142/S021820251440003X, URL <http://dx.doi.org/10.1142/S021820251440003X>.
- [22] F. Brezzi, R. S. Falk, L. D. Marini, Basic principles of mixed virtual element methods, *ESAIM Math. Model. Numer. Anal.* 48 (4) (2014) 1227–1240, ISSN 0764-583X, doi:10.1051/m2an/2013138, URL <http://dx.doi.org/10.1051/m2an/2013138>.

- [23] F. J. Gaspar, J. L. Gracia, F. J. Lisbona, C. W. Oosterlee, Distributive smoothers in multigrid for problems with dominating grad-div operators, *Numer. Linear Algebra Appl.* 15 (8) (2008) 661–683, ISSN 1070-5325, doi:10.1002/nla.587, URL <http://dx.doi.org/10.1002/nla.587>.
- [24] A. Brandt, Multi-level adaptive solutions to boundary-value problems, *Math. Comp.* 31 (138) (1977) 333–390, ISSN 0025-5718.
- [25] W. Hackbusch, Multigrid methods and applications, vol. 4 of *Springer Series in Computational Mathematics*, Springer-Verlag, Berlin, ISBN 3-540-12761-5, doi:10.1007/978-3-662-02427-0, URL <http://dx.doi.org/10.1007/978-3-662-02427-0>, 1985.
- [26] U. Trottenberg, C. W. Oosterlee, A. Schüller, Multigrid, Academic Press Inc., San Diego, CA, ISBN 0-12-701070-X, with contributions by A. Brandt, P. Oswald and K. Stüben, 2001.
- [27] P. Wesseling, An introduction to multigrid methods, Pure and Applied Mathematics (New York), John Wiley & Sons, Ltd., Chichester, ISBN 0-471-93083-0, 1992.
- [28] J. Xu, Iterative methods by space decomposition and subspace correction, *SIAM Rev.* 34 (4) (1992) 581–613, ISSN 0036-1445, doi: 10.1137/1034116, URL <http://dx.doi.org/10.1137/1034116>.
- [29] D. N. Arnold, R. S. Falk, R. Winther, Multigrid in  $H(\text{div})$  and  $H(\text{curl})$ , *Numer. Math.* 85 (2) (2000) 197–217, ISSN 0029-599X, doi: 10.1007/PL00005386, URL <http://dx.doi.org/10.1007/PL00005386>.
- [30] R. Hiptmair, J. Xu, Nodal auxiliary space preconditioning in  $\mathbf{H}(\text{curl})$  and  $\mathbf{H}(\text{div})$  spaces, *SIAM J. Numer. Anal.* 45 (6) (2007) 2483–2509 (electronic), ISSN 0036-1429, doi:10.1137/060660588, URL <http://dx.doi.org/10.1137/060660588>.
- [31] C. Rodrigo, F. J. Gaspar, F. J. Lisbona, Geometric multigrid methods on Triangular Grids: Application to semi-structured meshes, Lambert Academic Publishing, Saarbrücken, doi:10.1016/j.apnum.2009.01.003, URL <http://dx.doi.org/10.1016/j.apnum.2009.01.003>, 2012.
- [32] V. Girault, P.-A. Raviart, Finite element methods for Navier-Stokes equations, vol. 5 of *Springer Series in Computational Mathematics*,

- Springer-Verlag, Berlin, ISBN 3-540-15796-4, doi:10.1007/978-3-642-61623-5, URL <http://dx.doi.org/10.1007/978-3-642-61623-5>, theory and algorithms, 1986.
- [33] J.-C. Nédélec, Mixed finite elements in  $\mathbf{R}^3$ , *Numer. Math.* 35 (3) (1980) 315–341, ISSN 0029-599X, doi:10.1007/BF01396415, URL <http://dx.doi.org/10.1007/BF01396415>.
- [34] J.-C. Nédélec, A new family of mixed finite elements in  $\mathbf{R}^3$ , *Numer. Math.* 50 (1) (1986) 57–81, ISSN 0029-599X, doi:10.1007/BF01389668, URL <http://dx.doi.org/10.1007/BF01389668>.
- [35] P.-A. Raviart, J. M. Thomas, A mixed finite element method for 2nd order elliptic problems, in: *Mathematical aspects of finite element methods* (Proc. Conf., Consiglio Naz. delle Ricerche (C.N.R.), Rome, 1975), Springer, Berlin, 292–315. *Lecture Notes in Math.*, Vol. 606, 1977.
- [36] R. Wienands, W. Joppich, Practical Fourier analysis for multigrid methods, vol. 4 of *Numerical Insights*, Chapman & Hall/CRC, Boca Raton, FL, ISBN 1-58488-492-4, with 1 CD-ROM (Windows and UNIX), 2005.
- [37] F. J. Gaspar, J. L. Gracia, F. J. Lisbona, Fourier analysis for multigrid methods on triangular grids, *SIAM J. Sci. Comput.* 31 (3) (2009) 2081–2102, ISSN 1064-8275, doi:10.1137/080713483, URL <http://dx.doi.org/10.1137/080713483>.
- [38] F. J. Gaspar, F. J. Lisbona, C. Rodrigo, Multigrid Fourier analysis on semi-structured anisotropic meshes for vector problems, *Math. Model. Anal.* 15 (1) (2010) 39–54, ISSN 1392-6292, doi:10.3846/1392-6292.2010.15.39-54, URL <http://dx.doi.org/10.3846/1392-6292.2010.15.39-54>.
- [39] B. Gmeiner, T. Gradl, F. Gaspar, U. Råde, Optimization of the multigrid-convergence rate on semi-structured meshes by local Fourier analysis, *Comput. Math. Appl.* 65 (4) (2013) 694–711, ISSN 0898-1221, doi:10.1016/j.camwa.2012.12.006, URL <http://dx.doi.org/10.1016/j.camwa.2012.12.006>.
- [40] C. Rodrigo, F. Sanz, F. J. Gaspar, F. J. Lisbona, Local Fourier analysis for edge-based discretizations on triangular grids, *Numer. Math. Theor. Meth. Appl.*, in press, 2015.

- [41] S. P. MacLachlan, C. W. Oosterlee, Local Fourier analysis for multigrid with overlapping smoothers applied to systems of PDEs, *Numer. Linear Algebra Appl.* 18 (4) (2011) 751–774, ISSN 1070-5325, doi:10.1002/nla.762, URL <http://dx.doi.org/10.1002/nla.762>.
- [42] J. Molenaar, A two-grid analysis of the combination of mixed finite elements and Vanka-type relaxation, in: *Multigrid methods, III* (Bonn, 1990), vol. 98 of *Internat. Ser. Numer. Math.*, Birkhäuser, Basel, 313–323, doi:10.1002/nme.4626, URL <http://dx.doi.org/10.1002/nme.4626>, 1991.
- [43] S. Sivaloganathan, The use of local mode analysis in the design and comparison of multigrid methods, *Comput. Phys. Commun.* 65 (1991) 246–252, doi:10.1016/0010-4655(91)90178-N.
- [44] C. Rodrigo, F. J. Gaspar, F. J. Lisbona, On a local Fourier analysis for overlapping block smoothers on triangular grids, submitted, 2015.